Proceedings of the Third International Conference on Modeling, Simulation and Applied Optimization
Sharjah,U.A.E January 20-22 2009

Carbon Black production from thermal

Decomposition of Sub-quality Natural Gas

Mohammad Javadi

Ferdowsi University ofMashhad

Department of Mechanical Engineering
Mashhad, Iran

mohammad.javadi@gmail.com

Mohammad Moghiman

Ferdowsi University ofMashhad

Department of Mechanical Engineering
Mashhad, Iran

mmoghiman@yahoo.com

Mohammad.H Ghodsirad

Ferdowsi University ofMashhad

Department of Mechanical Engineering
Mashhad, Iran

ho_gh74@stu-mail.um.ac.ir

ABSTRACT

The objective of this paper is computational investigation of the carbon black production through thermal decomposition of waste gases containing CH_4 and H_2S, without requiring a H_2S separation process. The chemical reaction model, which involves solid carbon, sulfur compounds and precursor species for formation carbon black, based on an assumed Probability Density Function (PDF) parameterized by the mean and variance of mixture fraction and β-PDF shape. The effects of feedstock mass flow rate and reactor temperature on carbon black, S_2, SO_2, COS and CS_2 formation are investigated. The results show that the major factor influencing CH_4 and H_2S conversions is reactor temperature. For temperatures higher than $1100^{\circ}K$, the reactor CH_4 conversion reaches 100%, whilst H_2S conversion increases for temperatures higher than $1300^{\circ}K$. The results reveal that at any temperature, H_2S conversion is less than that of CH_4. The results also show that in the production of carbon black from sub-quality natural gas, the formation of carbon monoxide which is occurring in parallel, play a very significant role. For lower values of feedstock flow rate, CH_4 mostly burns to CO and consequently, the production of carbon black is low.

Keywords: Carbon black, sulfur compounds, thermal decomposition, sour natural gas

1. INTRODUCTION

As the prices of fossil fuel increase, abundant sour natural gas, so called sub-quality natural gas (SQNG) resources become important alternatives to replace increasingly exhausted reserves of high quality natural gases for the production of carbon black, hydrogen, sulfur and/or CS_2 [1– 3] . Gas flaring has also been blamed for environmental and health problems such as acid rain, asthma, skin and breathing problems [4, 5]. The removal of H_2S from SQNG is expensive and not commercially for large-scale plants. When H_2S concentration in natural gas is higher than about 1.0%, the high separation cost makes the SQNG economically unfeasible as an energy production source [1]. As mentioned above, the production of carbon black from SQNG is one possible option to use this wasted energy resource and reduce carbon and hydrogen sulfide emissions at the same time. In the practical carbon black furnace, turbulent thermal decomposition of CH_4+ H_2S feedstock produces carbon black, hydrogen and other sulfur compounds [6].

Carbon black is widely used as filler in elastomers, tires, plastics and paints to modify the mechanical, electrical and optical properties of materials in which they are dispersed and consequently determine their applications [8]. In the practical carbon black furnaces, the main process of carbon black production is oxidative thermal decomposition of feedstock hydrocarbon fuel [9].

The purpose of this paper is to analyze possibilities for efficient production of carbon black from sub-quality natural gas (SQNG) using a 3D numerical technique, which predicts detailed turbulent flame structure, carbon black formation and sulfur compounds production. The effect of relevant process parameters such as feedstock mass flow rate and reactor temperature on carbon black, S_2, SO_2, COS and CS_2 formation are investigated.

2. Gas furnace black and thermal decomposition of SQNG

The carbon black furnace used in this investigation is a small-scale axial flow gas furnace identical to that reported previously by Moghiman[10]. The furnace has been designed on the basis of using gaseous fuels as feedstock hydrocarbon, with a maximum output of 10 kg carbon black per hour. The basic geometry of the carbon black furnace is shown in Fig. 1, consisting of a precombustor, a mixing zone and a reactor. In the precombustor, the axially injected natural gas fuel burns with the process air, which is introduced through two tangential inlets. Then, the highly swirling hot gases meet the feedstock sub-quality natural gas fuel, which is injected radially into the precombustor in the vicinity of the mixing zone. The abrupt enlargement in diameter at the exit of the choke encourages the mixing of feedstock fuel with the hot gases [9].

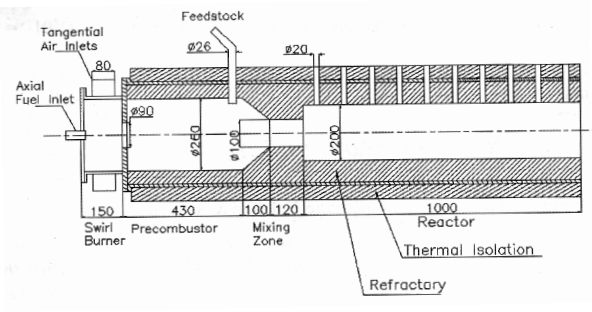

Fig. 1. Carbon black gas furnace

Turbulent rich combustion and thermal decomposition of CH_4+ H_2S feedstock fuel produces carbon black, sulfur compounds and other precursor species for the formation of carbon black.

3. Chemical reaction modeling

The production of carbon black through thermally decomposition of SQNG involved a complex series of chemical reactions which control the conversion of both $CH_4$and H_2S. The decomposition reaction of $CH_4$and H_2S are equivalent to [3, 12]:

$$CH_4 \rightarrow C(S) + 2H_2 \quad \Delta H^{\circ}_{298} = -74.9\,kJ/mol \qquad \text{Reaction (1)}$$

$$H_2S \rightarrow \frac{1}{2}S_2 + H_2 \quad \Delta H^{\circ}_{298} = -79.9\,kJ/mol \qquad \text{Reaction (2)}$$

Because reaction 1 is mildly endothermic, it requires temperatures higher than $850^{\circ}K$ to proceed at reasonable rate [13], and, as reaction 2 is highly endothermic, the temperatures must be above $1500^{\circ}K$ for achieving reasonable rate [6]. A portion of CH_4 and H_2S can be oxidized to produce CO, CO_2 and SO_2. H_2S also can react with CO_2 producing COS [14]:

$$H_2S + CO_2 \Leftrightarrow COS + H_2O \qquad \text{Reaction (3)}$$

Under special circumstances including using catalyst H_2S can react with methane producing carbon disulfide (CS_2) and H_2 [3].

$$2H_2S + CH_4 \Leftrightarrow CS_2 + 4H_2 \qquad \text{Reaction (4)}$$

4. Turbulence–chemistry interaction

The mixture fraction / PDF method is used to model the turbulent chemical reactions occurring in the diffusion, combustion and thermal decomposition of natural gas in the carbon black furnace. This method, which assumes the chemistry is fast enough for a chemical equilibrium to always exist at molecular level, enables the handling of large numbers of reacting species, including intermediate species. Transport equations are solved for the mean mixture fraction $\bar{f}$, its variance $\overline{f'^2}$ and for enthalpy $\bar{h}$. The chemistry calculations and the pdf integrations are performed using a preprocessing code, assuming chemical equilibrium between 30 different species. The results of the chemistry calculations are stored in look-up tables which relate the mean thermochemical variables (species mass fractions, temperature and density) to the values of $\bar{f}$, $\overline{f'^2}$ and $\bar{h}$ [15].

5. Numerical solution procedure

Fluent CFD software which allows one to model furnaces with complex geometry and solution-adaptive grid refinement is applied in this study to solve the 3D problem. Gambit preprocessor is used for the fully three dimensional geometry creations and unstructured grid generation. The 3D volume grid is represented in Fig 2. The domain is discretized into a grid of 20493 nodes and 82745 tetrahedral cells. The conservation equations of mass, momentum, energy, reynolds stresses, dissipation rate, mixture fraction and its variance, and concentration of soot are solved by applying a finite-volume treatment, using a second-order upwind scheme for discretisation of the convective terms of transport equations.

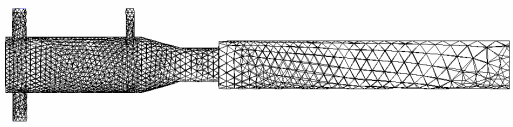

Fig. 2. Three-dimensional tetrahedral grid

The two-step Tesner soot model is applied within the finite-volume CFD code FLUENT. The two-step Tesner soot model [16] predicts the generation of radical nuclei and then computes the formation of soot on these nuclei. The radiative heat transfer in the absorbing, emitting and scattering medium is calculated by the Discrete Ordinates (DO) radiation model [17]. The RSM model is used for prediction of anisotropic, highly swirling and recirculating flow inside the combustor. The conventional wall-function approach is used in the near-wall region. At the inlet boundary, conditions are specified once and did not need updating during the course of the solution procedure. At the outlet boundary, zero gradient conditions are applied. A fixed temperature condition is applied at the wall of the furnace.

A grid dependence study is conducted to arrive at the appropriate size of the grid to combine accuracy and efficiency. The number of grid points is varied from 17231 to 36387 for typical set operating conditions. It is observed that the field quantities varied less than 1% after the number of grid points is increased beyond 20493. For the radiation model, emissivity coefficient at the flow inlets and outlets are taken to be 1.0 (black body absorption). Wall emissivity is set to be 0.6, a typical value for gas combustion.

5. Results

Numerical calculations are performed on the axial flow gas furnace used by moghiman [10] as shown in Fig. 1. The total precombustor inlet airflow rate is $19\times10^{-3}\,m^3/s$, at a temperature of 690Kand normal atmospheric pressure of 1 bar. The equivalence ratio used for the precombustor is 0.92. The accuracy of the quantitative or even the qualitative trends of the results relating to combustion and decomposition parameters depends on

the accuracy with which the temperature and species concentration fields are determined from the numerical calculation of the present model. To establish the accuracy of the present computation, a possible comparison between experimental measurements of Moghiman [10], with no H_2S, has been made with calculated results of this model. For comparison purposes, we first conducted computations without H_2S in feedstock mass flow rate.

A comparison of reactor outlet average temperature and carbon black yield (kg carbon black/kg feedstock) predicted by this study is made with the experimental results (Figs. 3 and 4). The comparison between predicted and measured temperatures (Fig. 3) reveals that the calculated results show lower temperatures than the experimental results especially for higher feedstock flow rate. The discrepancy between the two results can be due to the fundamental assumption made in the combustion model used (PDF fast chemistry combustion model) which assumes that chemistry is fast enough for a chemical equilibrium. Comparison between the computed and measured carbon black yield is shown in Fig. 4. It is seen that the predicted carbon black yield values have very good agreement with measurement results the maximum carbon black yield is accrued at equivalence ratio=3. The discrepancy between the two results can be attributed to the temperature levels obtained by the two methods (see Fig. 3). The lower temperature levels obtained by the computation method are due to higher decomposition of CH_4.

Fig. 5 presents the calculated distributions for CH_4, H_2S, temperature, soot, solid carbon, COS and gaseous sulfur for a 3×10^{-3} kg/s feedstock flow rate. H_2S mass fraction in natural gas is 10%. Of particular importance is Figs. 5d-f showing the formation of soot from incomplete combustion of entering methane and the production of solid carbon and gaseous sulfur from thermal decomposition of the methane- hydrogen sulfide jet interacting with hot surroundings. Clearly, the use of more inlets for feedstock methane-hydrogen sulfide injection would have improved flow and aero chemistry symmetry and, undoubtedly production of carbon black and sulfur compounds.

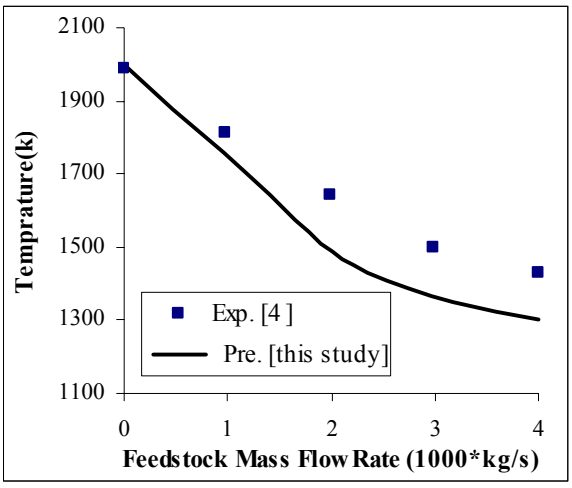

Fig. 3. Comparison of the predicted reactor outlet temperature with the experimental data

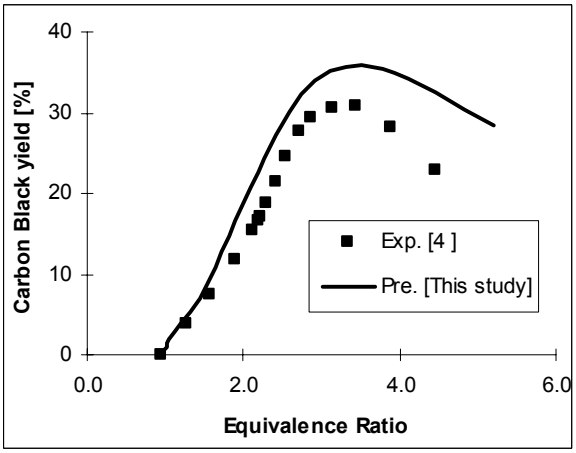

Fig. 4. Comparison of the predicted carbon black yield with the experimental data

Fig. 6 shows the variation of reactor outlet temperature as a function of feedstock mass flow rate for two conditions: a) with H_2S, b) without H_2S. It can be seen that the results of the two conditions are similar. The small discrepancy between the results of the two conditions is because the CH_4 decomposition reaction begins at lower temperature in comparison with the H_2S decomposition reaction. The figure reveals that temperatures sharply decrease with increasing feedstock flow rate because of the endothermic nature of both CH_4 and H_2S decomposition reaction.

Figs. 7 and 8 show the effect of feedstock flow rate and reactor outlet temperature on CH_4 and H_2S conversions. CH_4 and H_2S conversions are [3]:

$$CH_4 \text{ conversion} = \frac{[CH_4]_0 - [CH_4]}{[CH_4]_0} \times 100,$$

$$H_2S \text{ conversion} = \frac{[H_2S]_0 - [H_2S]}{[H_2S]_0} \times 100$$

where $[CH_4]_0$ and $[H_2S]_0$ denote the initial (input) concentration of CH_4 and H_2S, respectively. $[CH_4]$ and $[H_2S]$ are equilibrium concentration of CH_4 and H_2S at reactor outlet, respectively.

Fig. 7 reveals that the H_2S conversion sharply decreases with increasing feedstock flow rate; this attributed to the endothermic nature of feedstock H_2S and CH_4 decomposition.

For higher values of feedstock flow rate (≥ 0.002kg/s) CH_4 conversion decreases with increasing feedstock flow rate. This occurs because of the endothermic nature of CH_4 decomposition. The major factor influencing CH_4 and H_2S conversions is temperature. Fig. 8 shows that the CH_4conversion reactor reaches 100% as the reactor temperature become greater than 1100°K. Because CH_4 decomposition reaction is mildly endothermic, the temperature must be above 850°K for the reaction to proceed at a reasonable rate. This is accord with results of Hung and Raissi [3]. At any temperature, H_2S conversion is less than that of CH_4, especially at temperature below 1300°K wherein H_2S conversion is less than 5%. For higher values of reactor

temperature ($\geq 1300^{\circ}K$), H_2S conversion increases sharply with temperature. As H_2S decomposition reaction is endothermic, the temperature must be above $1500^{\circ}K$ for the reaction to proceed at a reasonable rate.

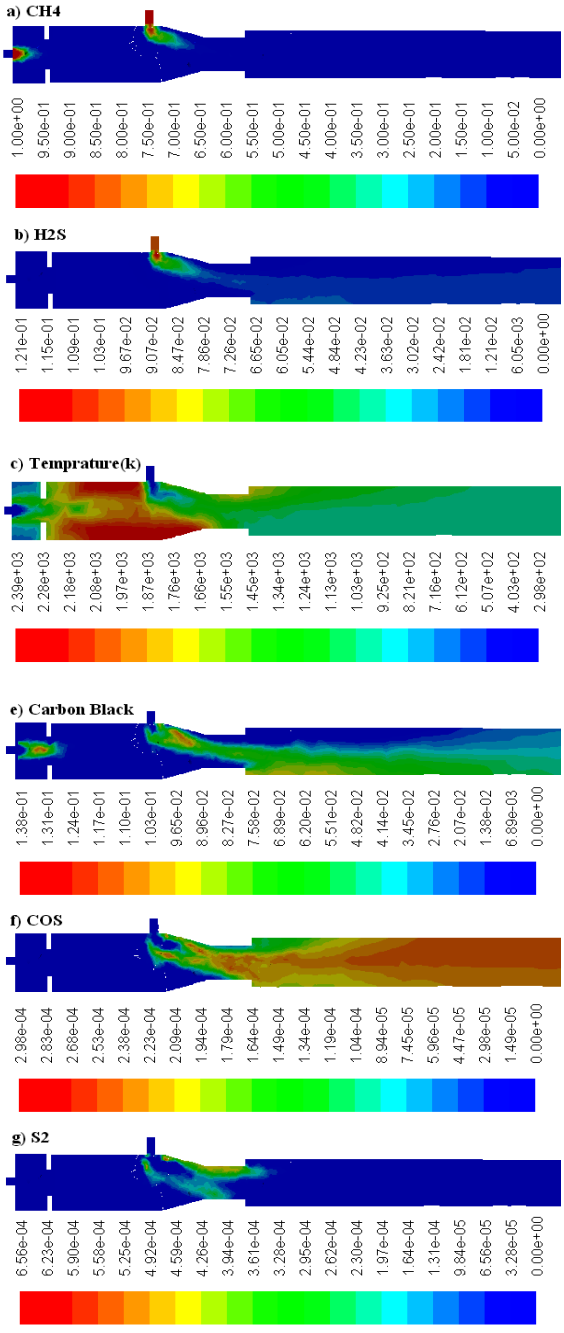

Fig. 5 . Contour of species mass fractions and temperature (K)

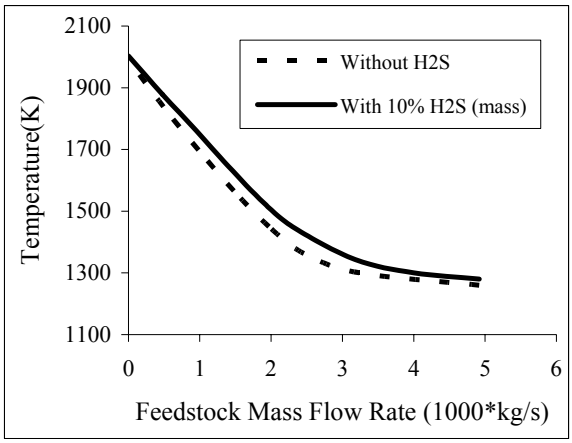

Fig. 6 Effect of feedstock flow rate on calculated outlet temperature

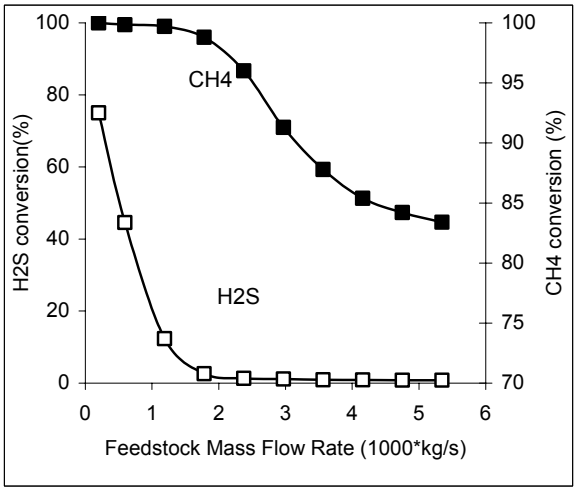

Fig. 7. Effect of feedstock mass flow rate on H_2S and CH_4 conversions

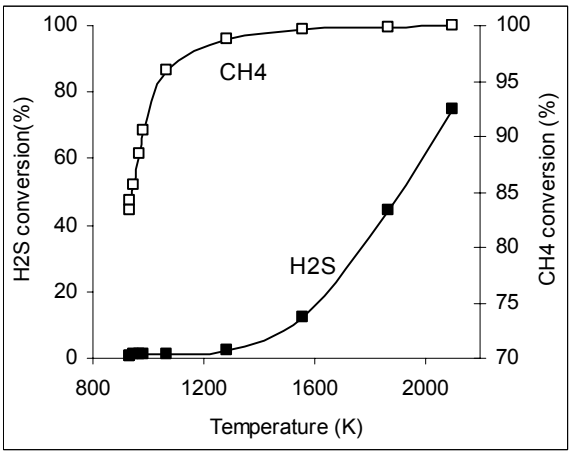

Fig. 8. Effect of reactor outlet temperature on H_2S and CH_4 conversions

Figs. 9 shows the effect of feedstock flow rate on CH_4, carbon black, soot and CO mass fractions at the outlet of the furnace. It can be seen that for lower values of feedstock, the very high temperature precombustor effluent (see Fig. 6) causes the feedstock hydrocarbon (CH_4) mostly burns to CO, consequently, the production of carbon black is low. For higher values of feedstock flow rate, the formation of carbon black increases, and, due to reduction of temperature, the formation of CO and soot decreases. Fig. 10 shows the variation of sulfur (given by decomposition of H_2S) and SO_2 (given by combustion of H_2S) yields as a function of feedstock flow rate at the outlet of the furnace. S_2 and SO_2 yields are defined as :

$$S_2(\%) = \frac{2[S_2]}{[H_2S]_0} * 100 \ , \ SO_2(\%) = \frac{[SO_2]}{[H_2S]_0} * 100 \ .$$

where $[S_2]$ and $[SO_2]$ denote the equilibrium molar concentrations for species S_2 and SO_2, respectively [6]. The figure reveals that for low values of feedstock flow rate ($\leq 0.002 kg/s$), due to high levels of temperature (see Fig. 3) H_2S mostly converts to S_2 and SO_2. It can be seen that for higher values of feedstock flow rate the formations of S_2 and SO_2 are too low. This is due to reduction of H_2S conversion (see Fig. 7).

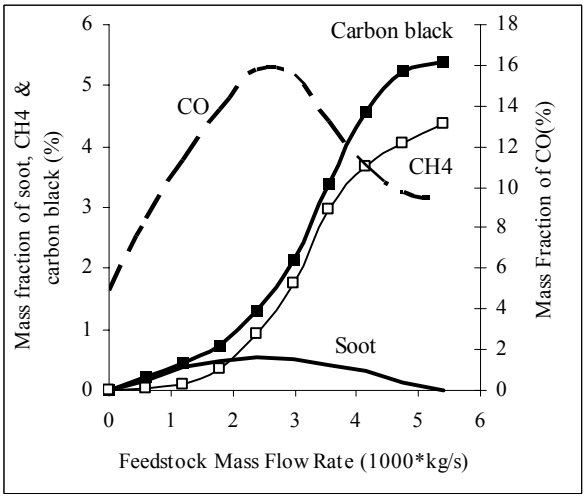

Fig. 9. Effect of feedstock flow rate on CH_4, CO, carbon black and soot mass fractions

Figs. 11 presents the effects of feedstock mass flow rate on yields of COS and CS_2, respectively. The yields of COS and CS_2 are defined as:

$$COS(\%) = \frac{[COS]}{[H_2S]_0} * 100 \ , \ CS_2(\%) = \frac{[CS_2]}{[CH_4]_0} * 100$$

where [COS] and $[CS_2]$ denote the equilibrium molar concentrations for species COS and CS_2, respectively [3]. Fig. 11 shows that the COS and CS_2 yields increase with increasing feedstock flow rate until the yields reach the maximum values, and then drop with further increase in the feedstock flow rate. Figs. 11 reveal that the amount of CS_2 is always low ($\leq 0.0007\%$). This is accords with results of C. Huang, A. Raissi [3] and G. P. Towler and S. Lynn [12].

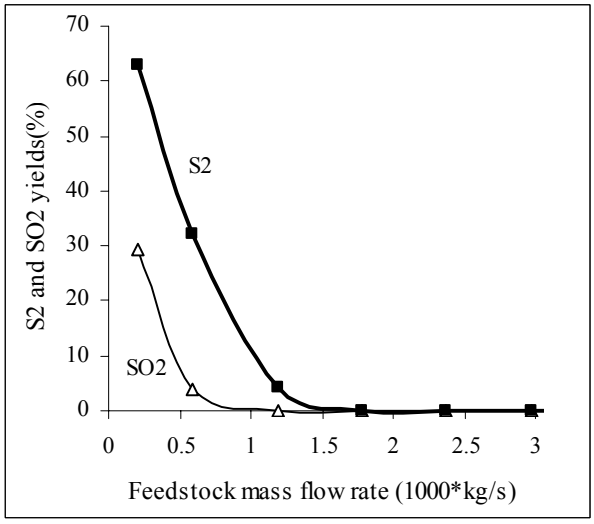

Fig. 10. Effect of feedstock mass flow rate on S_2 and SO_2

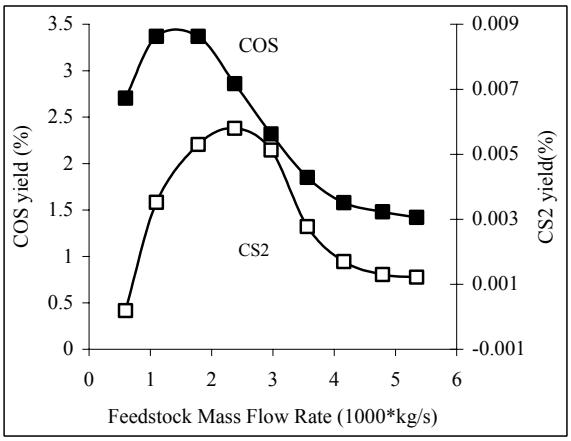

Fig. 11. Effect of feedstock mass flow rate on COS and CS_2 yield

6. Conclusions

The production of waste gases containing methane (CH_4) and hydrogen sulfide (H_2S) has been computationally investigated and fully analyzed. The process mainly involves the oxidative and thermal decomposition of CH_4 and H_2S. We also conducted some computations with no H_2S present in feedstock hydrocarbon to compare the results of this model with available experimental measurements. Based on the presented results, the following conclusions may be drawn:

- The major factor influencing CH_4 and H_2S conversions is reactor temperature.
- For temperatures higher than $1100^\circ K$, the reactor CH_4 conversion reaches 100%.

- At any temperature, H_2S conversion is less than that of CH_4, especially at temperature below $1300^{\circ}K$ wherein H_2S conversion is less than 5%.
- For temperatures higher than $1300^{\circ}K$, H_2S conversion increases sharply with temperature. The major products of the processes are $S_2$and SO_2 while carbonyl sulfide (COS) and carbon disulfide (CS_2) are minor products within this temperature range.
- For lower values of feedstock flow rate, CH_4 mostly burns to CO and consequently, the production of carbon black is low. For higher values of feedstock, the formation of carbon black increases to a maxima.

7. Refrences

[1] C. Huang, A. T-Raissi, Thermodynamic analyses of hydrogen production from sub-quality natural gas, Part I: Pyrolysis and autothermal pyrolysis, *Power Sources,* Vol.163, 2007, pp. 645–652.

[2] H. K. Abdel, M. A. Shalabi, D. K. AL-Harbi and T. Hakeem, Non catalytic partial oxidation of sour natural gas, Hydrogen Energy, Vol. 23, 1998, pp. 457-462.

[3] C. Huang, A. T-Raissi, Liquid hydrogen production via hydrogen sulfide methane reformation, power sources, Vol.175, 2008, pp. 464-472.

[4] T. M. Gruenberger, M. Moghiman, P. J. Bowen, N. Syred, Improving mixing behaviour in new design of carbon black furnace using 3D CFD modeling, 5th European conference on industrial furnaces and boilers, Portugal, 2000.

[5] T. W. Lambert, V. M. Goodwin, D. Stefani, L. Strosher, Hydrogen sulfide (H2S) and sour gas effects on the eye. A historical perspective, Science of the Total Environment, Vol. 367, 2006, pp.1–22.

[6] C. Huang, A. T-Raissi, Thermodynamic analyses of hydrogen production from sub-quality natural gas, Part II: Steam reforming and autothermal steam reforming, Power Sources, Vol. 163, 2007, pp.637–644.

[7] U. Ghosh, The Role of Black Carbon in Influencing Availability of PAHs in Sediments, Human and Ecological Risk assessment, Vol. 13, pp. 276-285, 2007.

[8] W. Cho, S. H. Lee, W. S. Ju, Y. Baek, J. K. Lee, Conversion of natural gas to hydrogen and carbon black by plasma and application of plasma carbon black, Catalysis Today, Vol. 98, 2004, pp. 633–638.

[9] F. C. Lockwood, J. E. Niekerk, J. E. Van, Parametric study of a carbon black oil furnace, Combustion and Flame, Vol. 103, 1995, pp. 76-90.

[10] M. Moghiman, Numerical prediction and measurement of carbon black through turbulent combustion and decomposition of natural gas, Scientia Iranica, Vol.10, 2003, pp.211-219.

[11] T. M. Gruenberger, M. Moghiman, P. J, Bowen, N. Syred, Dynamic of soot formation by turbulent combustion and thermal decomposition of natural gas, Combustion science and technology Vol.174, 2002, pp.67-86.

[12] P. Towler, S. Lynn, Sulfur recovery with reduced emissions, low capital investment and hydrogen co-production, Chemical engineering communications, Vol. 155, 1996, pp. 113-143.

[13] A. M. Dunker, S. Kumar, P. A. Mulawa, Production of hydrogen by thermal decomposition of methane in a fluidized-bed reactor—Effects of catalyst, temperature, and residence time, Hydrogen Energy, Vol.31, 2006, pp. 473-484.

[14] K. Sakanishi, Z. Wu, A.Matsumura, I. Saito, Simultaneous removal of H2S and COS using activated carbons and their supported catalysts, Catalysis Today, Vol.104, 2005, pp.94–100. [15] A. Saario, A. Rebola, Heavy fuel oil combustion in a cylindrical laboratory furnace: measurements and modeling, Fuel, Vol.84, 2005, pp.359–369.

[16] P.A. Tesner, T. D. Snegiriova, and V. G. Knorre. Combustion and Flame, 17, 253-260, (1971).

[17] W. P. Jones and J. H. Whitelaw, Calculation Methods for Reacting Turbulent Flows: A Review. Combustion and Flame, 48:1-26, 1982.